J Solid State Electrochem (2001) 5: 1–7 

ORIGINAL PAPER

C. Bohnke · J.L. Fourquet · N. Randrianantoandro
T. Brousse · O. Crosnier

# Electrochemical intercalation of lithium into the perovskite-type $NbO_2F$: influence of the $NbO_2F$ particle size

Received: 29 September 1999 / Accepted: 3 December 1999

**Abstract** Niobium(V) oxyfluoride, $NbO_2F$, has a perovskite structure and presents the property of lithium intercalation by topotactic chemical reaction either with n-butyllithium dissolved in n-hexane or by electrochemical reaction. The intercalation leads to the reduction of the transition metal from the oxidation state Nb(V) to the oxidation state Nb(III). This allows a theoretical $Li/NbO_2F$ intercalation ratio of 2. In this paper we will show that this theoretical value can be approached by using micron the sized active material particles. Moreover, the electrical properties of the cathode studied by the galvanostatic intermittent titration technique and a.c. impedance spectroscopy are explained in terms of structural and grain size considerations. Results of cycling experiments are also described.

**Key word** Oxyfluoride · Perovskite · Intercalation · Impedance spectroscopy · Galvanostatic intermittent titration technique

## Introduction

The crystallographic structure of $NbO_2F$ is shown in Fig. 1; it is isomorphous with $ReO_3$. This oxide structure can be described by a cubic unit cell with $a = 3.9048$ Å with the *Pm3m* space group [1]. It is built up of corner-sharing octahedra $NbX_6$ (X = O, F) that enclose a 12-coordinated A site. These A sites, which are totally empty, are located at the body center of a cube formed by the centers of eight octahedra. The size of these A sites is larger than the size of $Li^+$ ions.

The chemical intercalation of lithium into $NbO_2F$ by reaction with n-butyllithium in hexane has been already reported. The maximum lithium uptake of 2 Li per/Nb [if we consider a reduction of Nb(V) to Nb(III)] was obtained by Murphy et al. [2] at 50 °C. This material was tested as the cathode in a lithium battery by Renou [3]. In this work, the author showed the results of diffraction analysis on the chemical intercalated material. According to this author, the cubic phase $\alpha$-$Li_xNbO_2F$, which exists for $0 \le x < 0.15$ and is an isotype of $NbO_2F$, undergoes a small distortion which leads to the $\beta$-$Li_xNbO_2F$ phase. For $x > 0.5$ the $\beta$ phase transforms into a $LiNbO_3$-like structure with hexagonal symmetry. This transformation is completed for $x = 1.4$. Permer [1–4] has also shown by high-resolution transmission electron microscopy (HRTEM) in that the $\beta$ phase is a distortion of the initial $\alpha$-$NbO_2F$ phase, and transformation of the distorded cubic structure into a $LiNbO_3$-like structure with hexagonal symmetry occurs around $x \approx 0.6$ and is complete for $x = 1.6$. In the previous paper [5], we presented the discharge curve obtained by the galvanostatic intermittent titration technique (GITT) and the impedance spectra obtained during the intercalation process for a cathode material prepared by pressing carbon powder, unground $NbO_2F$ powder and PTFE. The maximum intercalation ratio was only 1.2 (60% of the expected maximum). The aim of this paper is to show the results obtained with micron-sized particles obtained by ball milling $NbO_2F$ (dimension of 2 μm or less). A model using an equivalent electrical circuit including only resistances, constant phase and diffusion Warburg elements was used.

C. Bohnke (✉) · J.L. Fourquet
Laboratoire des Fluorures, UPRES A6010,
Faculté des Sciences, Avenue O. Messiaen,
72085 Le Mans Cedex 9, France
e-mail: claude.bohnke@fluo.univ-lemans.fr

N. Randrianantoandro
Laboratoire de Physique de L'Etat Condensé,
UPRES A6087, Faculté des Sciences, Avenue O. Messiaen,
72085 Le Mans Cedex 9, France

T. Brousse · O. Crosnier
ISITEM, Laboratoire de Génie des Matériaux,
Rue Christian Pauc, BP 90604,
44306 Nantes Cedex 3, France

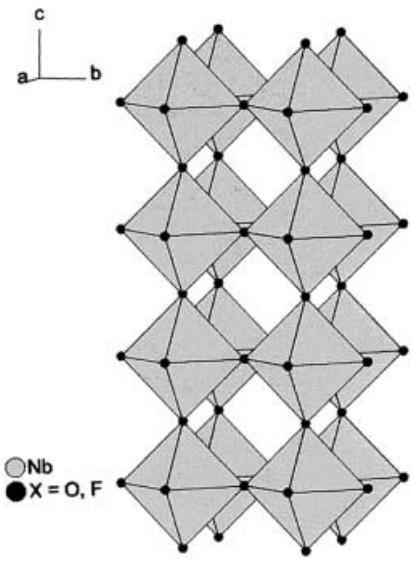


**Fig. 1** Crystal structure of $NbO_2F$ (X = O, F are statically distributed)

## Experimental

### Synthesis of $NbO_2F$

$NbO_2F$ was obtained by dissolution of $Nb_2O_5$ in HF (aq. 48%) followed by evaporation to dryness. This powder was heated in gold crucible at 100 °C under vacuum. The control of the purity of the product was made by X-ray powder diffraction (XRD) with a Phillips 1130 diffractometer using Cu $K_\alpha$ radiation and a vertical holder.

### Electrochemical insertion

Lithium intercalation was studied by galvanostatic discharge and the complex impedance technique with a Solartron 1260 FRA and an electrochemical interface Solartron 1287 connected to an AST Bravo computer. The electrochemical cell was a three-electrode setup with two lithium foils for counter and reference electrodes. The working electrode was a pellet ($s = 0.2$ cm$^2$ and about 3 mm thickness) obtained by pressing a mixture of $NbO_2F$ powder, graphite powder and PTFE in proportions 50:25:25 (% in weight). The quantity of $NbO_2F$ was about 30–50 mg. The electrolyte was a solution of dehydrated $LiClO_4$ dissolved in anhydrous propylene carbonate (0.1 mol/L$^{-1}$). The discharge curve was obtained by applying a constant current (either 20 or 5 μA during 2 h) and 18 hours of relaxation. After this time, the values of the equilibrium potential were constant and the quasi equilibrium was reached. The duration of the GITT experiment was about one month. The minimum potential was continuously checked not to go below 0 V/Li, in order to prevent the Li plating onto the sample. After 18 h of relaxation, the impedance spectra at different insertion ratios were measured with a 10 mV (rms) applied voltage. The typical-high frequency limit was 100 kHz and the low-frequency limit was 0.025 or 0.010 Hz.

### Particle milling

$NbO_2F$ powder was ballmilled with a Fritsch P7 planetary mill in a zirconium oxide jar with zirconium oxide balls during 1 h. The proportion of $NbO_2F$/ballweight was 48.5/1000. The weight of $NbO_2F$ was about 1 g. When no liquid was used (air grinding) there was no decrease of grain size, but when ethanol was added to the powder the decrease of grain size was significant. The XRD pattern showed no structural modification between the nontreated product and the milled product. However, after milling, the diffraction peaks were broader owing to a slight amorphization of the material.

### Particle size measurements

The particle sizes were measured with a Coulter laser granulometer in water. The determination was based on the spherical particle model of Fraunhofer. This model gives the specific surface and the stastistical size distribution of the particles. The results are obtained with the condition of a refractive index and a density of particles of 1. Consequently, the values are not absolute but permit us to compare the effect of milling. The particles before milling had a mean size of 9.5 μm (in volume) with a high percentage of 40 μm diameter particles. After evaporation of ethanol, the milled particles had a mean diameter of 1.2 μm (in volume) with two peaks at 0.3 μm and 3 μm. The ratio of the specific surface after and before milling was 3.07.

### Cycling measurements

#### *Cathode preparation*

$NbO_2F$ was tested as the cathode material in a lithium battery at the Laboratoire du Génie des matériaux, ISITEM, Nantes. The cathode was obtained by mixing the ground particles of $NbO_2F$, PVDF (polyvinylidene fluoride) and carbon black in the proportions 85:10:5 (% in weight) and dissolution in *N*-methyl-2-pyrrolidone. The homogeneous mixture was coated on a copper foil with a bare coater. The film was obtained after evaporation of the solvent at 70 °C during 1 h.

#### *Cycling experiments*

Cycling was performed in a glove box with a MacPile II multipotentiostat. The working electrode was a disk of cathode material (12 mm in diameter). A lithium metal foil was used as both counter and reference electrode. A glass fiber film wetted by the liquid electrolyte was used as a separator between the two electrodes. The electrolyte was $LiPF_6$ (1 M) in a mixture of ethylene carbonate-diethyl carbonate (2:1 by volume). Experiments were performed in the potentiostatic mode with a scan rate of 10 mV/10 s (terminology used in MacPile program) between 0.5 and 3.5 V/Li with 1.5 mg of active material. $I = f(E)$ curves are corrected from the ohmic drop.

## Results

### Discharge curves

The discharge curves for $NbO_2F$ obtained by the GITT method are shown in Fig. 2 for both ground and unground powders. Both curves display a similar shape: first, a smooth decrease of the potential as intercalation proceeds and then a sudden decrease followed by a plateau corresponding to the existence of a two-phase domain. The onset and the length of this plateau are dependent on the grain size of the lithiated material. Indeed, for ground oxide the two-phase plateau occurs

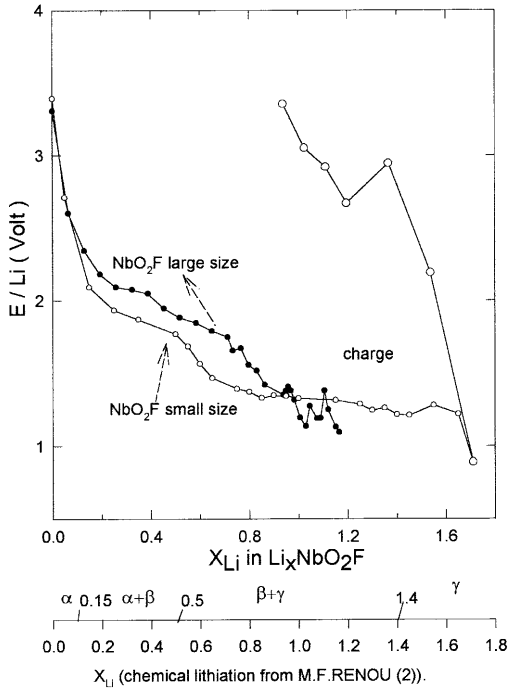


**Fig. 2** Galvanostatic intermittent titration technique curves for $NbO_2F$/C/PTFE electrodes in $LiClO_4$ (0.1 mol $L^{-1}$) propylene carbonate electrolyte. The *additional axis* indicates the structural transformations observed by X-ray diffraction with chemically intercalated materials. ○ $NbO_2F$ after mechanical grinding in ethanol; • $NbO_2F$ after synthesis

for $0.8 < x_{Li} < 1.6$, although for unground oxide it begins around 0.4. The smooth decrease indicates that for $0 < x_{Li} < 0.6$ and for $0 < x_{Li} < 0.4$ the lithium intercalation into ground and unground powders respectively occurs without structural change. At $x_{Li} = 0.6$ (or $x_{Li} = 0.4$) the oxide undergoes a structural transformation which is completed at $x_{Li} = 1.6$. These results differ slightly from those of Renou [3] and Permer [1, 4]. Renou suggested, from XRD results, the appearance of three phases as intercalation proceeds (see Fig. 2). The first phase for $0 < x < 0.15$, named $\alpha$-$Li_xNbO_2F$, is an isotype of $NbO_2F$ without any cell parameter change. For $0.15 < x < 0.5$ the cubic cell undergoes a small distortion, which leads to the $\beta$-$Li_xNbO_2F$, as named by Renou [3]. This distortion causes a small decrease of the cubic unit cell because the perovskite A-sites are too large to host the small $Li^+$ ions. The shrinkage of the holes is accomplished by a tilt of the $NbX_6$ octahedra. At $x = 0.5$ the distorted cubic structure of $Li_xNbO_2F$ begins to transform into a $LiNbO_3$-like structure with hexagonal symmetry. In her study of chemically lithiated $NbO_2F$, Permer observed shrinkage of the cubic unit cell at the beginning of the intercalation and it is clearly a structural transformation. For this author the transformation from the $NbO_2F$ to the $LiNbO_3$ structure type can be understood as a continuation of the tilt of the $NbX_6$ octahedra that starts as soon as some Li is introduced into the host structure [4]. For $x > 1.3$, this transformation is almost completed. Such a result would lead to the presence of a two-phase domain in a large $x_{Li}$ range going from the onset of the intercalation to 1.3. This assumption is supported by the HRTEM observations of this author [4]. The discharge curves obtained in this work are more consistent with Renou's interpretation. Our results seem to show that the beginning of the electrochemical intercalation (up to $x_{Li} = 0.6$) is not accompanied by a structural change of the host oxide but only by a distortion of the unit cell. The transformation from the distorted cubic cell to the $LiNbO_3$-like structure occurs around $x_{Li} \approx 0.6$ and is completed for $x_{Li} = 1.6$.

The size of the particles plays a role in the maximum lithium uptake, the values of the insertion ratio for the beginning of the structural transformation and also in the electrical connection between the grains during the intercalation. The maximum Li content is found to be 1.2 Li/Nb (60% of the expected maximum) and 1.6 Li/Nb (80% of the expected maximum) for unground and ground materials, respectively. The stuctural transformation occuring at $x_{Li} = 1.6$ leads to the irreversibility of the intercalation reaction. The injected charge during the discharge process is about 8.1 C (intercalation) and the injected charge during the charge process (deintercalation) is 2.4 C. This leads to about 28% reversibility only. The particle size has also an influence on the stability of the measurements, especially for high lithium content as shown in Fig. 2. Better stability may be due to a better electrical connection between the carbon grains and the micron-sized $NbO_2F$ particles.

## Impedance measurements and electrical model

Figure 3 shows typical impedance diagrams in the Nyquist plane recorded under open-circuit conditions after complete relaxation of the electrode. The data presented in this figure are relative to the electrode made of micron-sized particles. It has to be noted that the shape of the diagrams obtained with unground powder is very similar to the one shown in Fig. 3. Three frequency domains can be distinguished: the high-frequency domain well represented by an arc, the low-frequency domain which displays a linear behavior, and an intermediate frequency domain around 1 Hz which is more difficult to visualize.

The high-frequency arc can be ascribed to the charge transfer reaction at the electrode/electrolyte interface. This electrochemical reaction is characterized by a resistance $R_t$ associated with the double-layer capacitance of this interface. The low-frequency straight line is typical of a system under diffusion control and can be ascribed to the diffusion process of the $Li^+$ ions into the bulk of the oxide. It is characterized by a Warburg impedance ($W$). The intermediate frequency domain of the diagrams is related to a relaxation process with a higher time constant than the electrochemical charge transfer. It can be associated with the formation of a high intercalated film in the grain surface of $NbO_2F$ as the

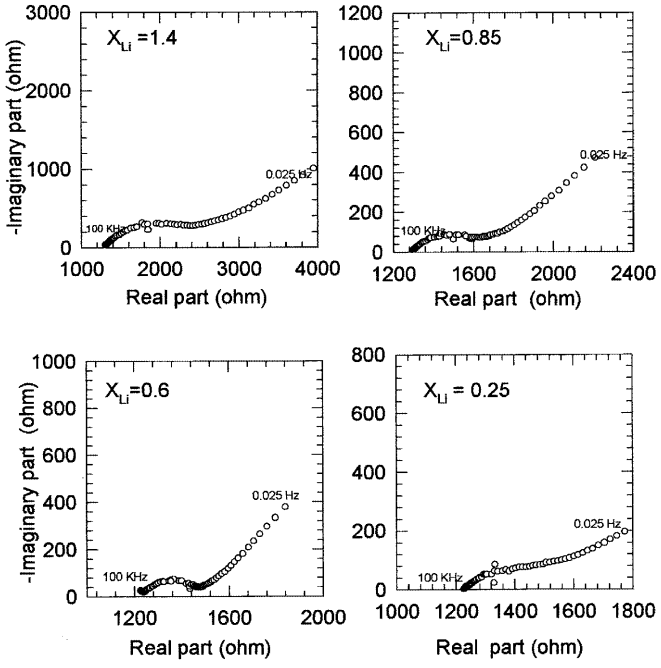


**Fig. 3** Impedance spectra obtained at equilibrium with $NbO_2F$/C/PTFE electrodes in $LiClO_4$ (0.1 mol $L^{-1}$) propylene carbonate electrolyte at various intercalation rate (ground particles). Applied voltage: 10 mV rms

intercalation proceeds. This domain of the diagrams (around 1 Hz) would be the signature of the inhomogeneity of the intercalated grains. Such a film can be electrically characterized by a resistance $R_2$ and a capacitance counting for the dielectric properties of the film. The formation of this high intercalated film is supported by the HRTEM observations made by Permer [1, 4]. Indeed, this author has clearly shown that during intercalation the diffusion of $Li^+$ ions into the host matrix starts from the surface to the bulk of the oxide grains, leading to inhomogeneous particles. The HRTEM image of an intercalated crystal fragment shows a relatively well-ordered cubic structure surrounded by a layer close to the surface where the atoms are arranged in a hexagonal pattern, which corresponds to the $LiNbO_3$-type structural compound. In order to take into account the different processes which take place during the electrochemical intercalation, we propose to use the electrical model shown in Fig. 4. This model involves the ohmic resistance $R_e$ made up of the electrolyte and the electrode resistances, the charge transfer reaction characterized by its resistance $R_t$, the formation of the surrounding layer characterized by its resistance $R_2$ and the diffusion process into the bulk of the material by a Warburg element $W$. To take into account the electrical inhomogeneities of the electrode, we used two constant-phase elements (CPE1 and CPE2) instead of pure capacitances for the double layer and high intercalated film, respectively. The impedance of a constant phase element is given by:

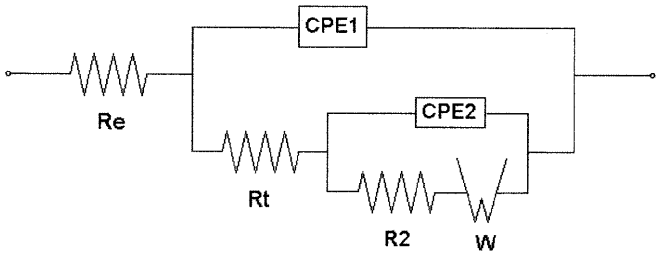


**Fig. 4** Equivalent circuit for an electrochemical process characterized by a charge transfer reaction-high inserted film formation-diffusion sequence

$$Z_{\mathrm{CPE}} = \frac{s}{(j\omega)^m} \tag{1}$$

For a pure capacitance, $s = 1$ and $m = 1$; $1/s$ has the dimension of a capacitance and can be viewed as a pseudo capacitance. The physical interpretation of the CPE is a transmission line with resistances and capacitances in a heterogeneous material and not a perfect electrical double layer, which is observed with a plane metallic electrode in contact with a liquid electrolyte. The insertion reaction modifies the electronic density in $NbO_2F$ particles and for this reason can give values of $s_1$ and $s_2$ that are not constant [6]. The fitting between the experimental data and this model has been obtained by using a Sygma plot program (Jandel Scientific). The value of $m$ for both CPEs is 0.46 and $s_1$ and $s_2$ are adjusted during the fitting procedure. No reliability factors are obtained but it is obvious that our model fits both the shape of the Nyquist plot and also the frequencies. The fitting procedure leads to the determination of the kinetics parameters of the electrochemical process (i.e. the exchange current is the inverse of the charge transfer resistance). An example of a fitting result is shown in Fig. 5 for $x_{\mathrm{Li}} = 0.75$. The black dots are the experimental data and the white ones are the fitted data obtained with the parameters mentioned in the graph.

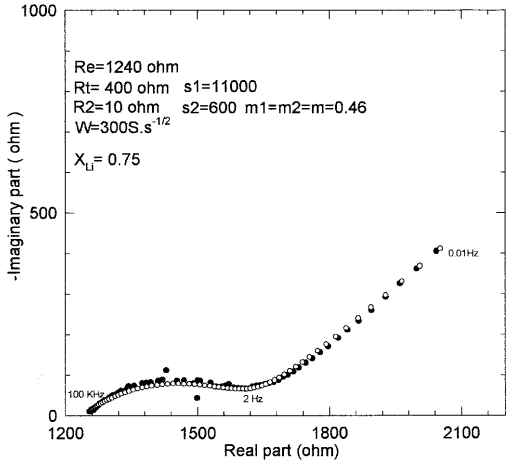


**Fig. 5** Impedance spectrum calculated with the electrical equivalent model (open circles) and experimental spectrum (solid circle) at the same frequencies for the $NbO_2F$/C/PTFE electrodes in $LiClO_4$ (0.1 mol $L^{-1}$) propylene carbonate electrolyte

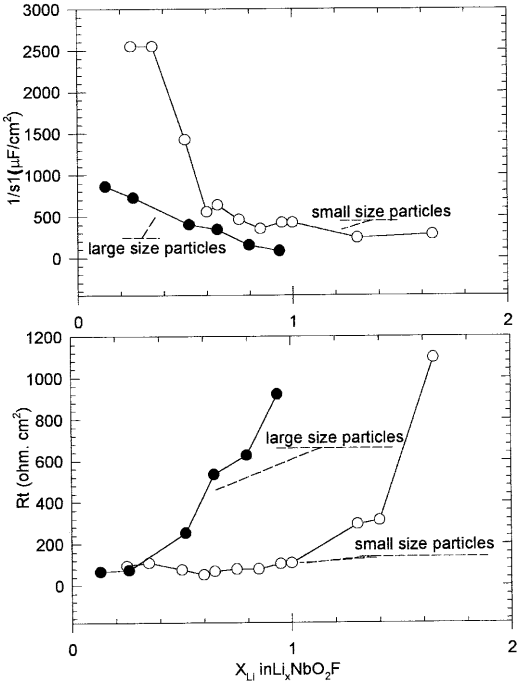


**Fig. 6** Variation of the charge transfer resistance and the parameter $1/s_1$ as a function of the intercalation ratio $x_{Li}$

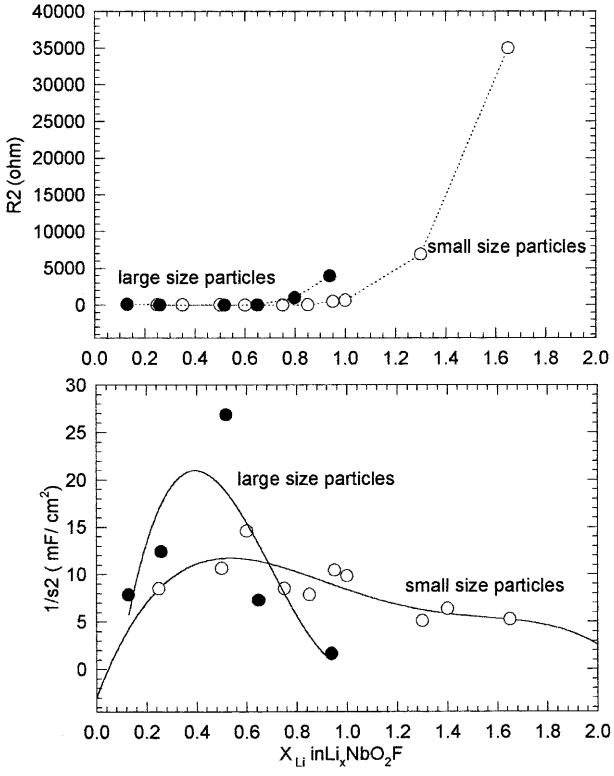


**Fig. 7** Variation of the $R_2$ resistance and $1/s_2$ as a function of the intercalation ratio $x_{Li}$

$W$ represents the Warburg prefactor value coming from the impedance of the Warburg diffusion:

$$Z_W = W(1-j)\omega^{-1/2} \quad (2)$$

The fitting procedure was applied at all impedance measurements at the different insertion ratios.

The variations of the electrical parameters as a function of the intercalation ratio $x_{Li}$, for both ground and unground materials, are shown in Figs. 6 and 7 for the charge transfer reaction and the high intercalated film formation, respectively. Figure 8 presents the variation of the high-frequency resistance. We have to note that for $0.2 < x_{Li} < 0.7$ the low-frequency domain of the impedance diagrams fitting gave a small value of $R_2$ and a contribution of the Warburg element. On the other hand, for high $x_{Li}$ values the value of $R_2$ becomes more and more important and the contribution of the Warburg element becomes negligible in the frequency domain investigated. Moreover, the determination of the Warburg prefactor did not allow us to calculate the diffusion coefficient of $Li^+$ by the formula of Ho et al. [7] because of the existence of a two-phase domain.

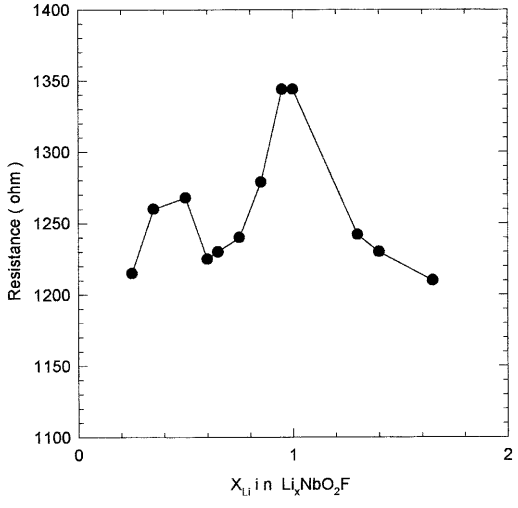


**Fig. 8** Variation of the high-frequency resistance as a function of the intercalation ratio $x_{Li}$

## Cycling measurements

The $i = f(E)$ curve during 10 cycles is shown in Fig. 9. The curve is characteristic for the intercalation-deintercalation process, as in $WO_3$ thin films [8]. Up to 2 V/Li in the cathodic part of the curve we can observe a smooth decrease of the potential. From 2 V the potential decreases suddenly to reach a plateau around 1.2 V/Li. This behavior is the same as observed in Fig. 2 and corresponds to the transformation from a disordered cubic phase to the hexagonal phase. During anodic polarization the reversibility of the two reactions is observed. The test for 50 cycles shows similar shapes with no important modifications of the electroactive material. After the first cycle, the intercalation is inefficient and

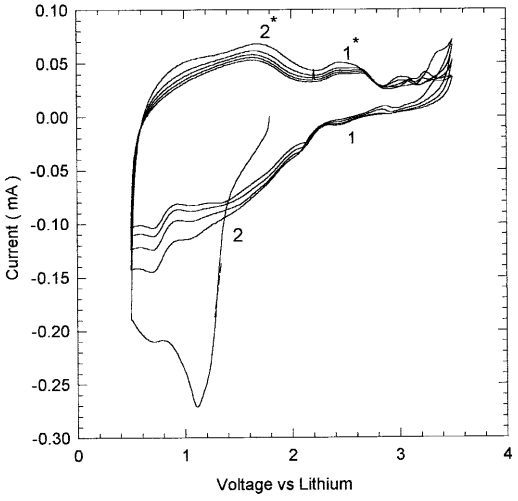


**Fig. 9** Cycling experiment of a battery with a thin film cathode of ballmilled particles of $NbO_2F$. Number of cycles: 10. Scan rate: 10 mV/10 s (MacPile II)

leads to very low values for the intercalation ratio. The capacity of this battery is of the order of 50 mAh/g.

## Discussion

From a general point of view the intercalation reaction can be described as a diffusion process in which lithium ions penetrate into the bulk of an active material. At the same time, electrons enter the material and reduction of the transition metal occurs. Since the ionic diffusion starts from the surface of the active particles, the outermost parts of the grains will contain more lithium than the central parts. If the intercalation proceeds without any change of the host structure, it can be assumed that homogeneity of the grain will occur slowly by diffusion. On the other hand, if the intercalation process alters the host structure, the entire particles may not be homogeneously intercalated and totally transformed into a new structure type even after relaxation. Such an inhomogeneity may explain some of the observed phenomena, especially the impedance data, the partial reversibility of the intercalation, and the influence of the particle size. The existence of inhomogeneous particles has been clearly shown by the HRTEM observations made by Permer [4] during lithiation of $NbO_2F$. We can assume that the same process occurs during the electrochemical reaction. The entire intercalation process occurring during discharge would then be characterized by an electrode reaction–high inserted film formation–diffusion sequence. In our experiments we can see that for a low intercalation ratio the resistance of the inserted film is small and diffusion can be observed. On the other hand, for a high intercalation ratio the resistance of the film increases abruptly and the diffusion is no longer observed. At the same time, the transfer resistance increases (Fig. 6). The occurrence of this phenomenon depends on the size of the active particles. For large particles, the structural transformation from the distorted cubic structure to the hexagonal one occurs around $x_{Li} = 0.4$ (Fig. 2). This corresponds to the increase of both the charge transfer and the $R_2$ resistances. For micron-sized particles the structural transformation occurs for a higher insertion ratio ($x_{Li} = 0.6$) as well as the increase of $R_t$ and $R_2$ (Figs. 6 and 7).

We can then assume that for low lithium content the particles consist of the original structure with a shell of a distorted cubic structure not very different electrically from the original one. Ionic diffusion occurs in these particles and a better reversibility of the insertion may be observed, as shown in Fig. 9 during cycling experiments. When $X_{Li}$ increases ($x_{Li} > 1$) the outermost part of the grains transforms to the hexagonal structure, leading to very inhomogeneous particles. The lithium diffusion through the interface of the two different structures becomes difficult and even impossible, strains build up within the grain and may lead to cracks. Such a phenomenon may explain the irreversibility of the *insertion* shown in Fig. 2. Such a process may be a general one, encountered when structural change occurs during an intercalation reaction.

The variation of high-frequency resistance is linked to the presence of the liquid electrolyte. If we assume $\sigma_{electrolyte} = 2.10^{-3}$ S cm$^{-1}$, $l = 0.5$ cm (distance between the working electrode and reference electrode), and $s = 0.196$ cm$^2$, the electrolyte resistance is about 1275 Ω. The high-frequency (hf) resistance is from the same order at the first stage of insertion (1240 Ω). We observe a variation of hf resistance from 10 to 50 Ω with a maximum for $x_{Li} = 1$. For $x_{Li} = 1.6$, the hf resistance become at about the starting value. With another fitting procedure (ZView Scribner/Solartron), the variations of $R_{hf}$ are of the same order of magnitude. This result can be interpreted by the variation of the geometrical factor of the electrode in contact with the electrolyte. The negative polarization of the working electrode makes easier the migration of the electrolyte into the porous structure of the composite electrode and increases the amount of electrolyte in contact with the carbon particles.

The electrochemical insertion of lithium in these materials leads to the progressive amorphization of the material as the insertion proceeds [9]. Recently, the existence of a film on an electroactive insertion compound was also observed with $Li_xCoO_2$ [10].

## Conclusion

$NbO_2F$ can be regarded as a model for lithium insertion into materials with a perovskite structure. The interpretation of both the discharge curves and the impedance spectroscopy diagrams is greatly facilitated by the contribution of HRTEM microscopy [2] and powder XRD analysis performed on these chemically inserted materials. The kinetics parameters obtained from

impedance spectroscopy are sensitive to the variation of the microscopic structure of the composite electrode as the insertion proceeds. In $NbO_2F$ the appearance of a two-phase domain is clearly shown. The low-frequency part of the impedance diagrams can be ascribed to the formation of a layer of high inserted compound surrounding a distorted cubic grain. It may be represented by an electrical equivalent circuit including a charge transfer resistance in parallel with the first constant phase element and the second resistance associated with a second constant phase element. The evolution of the high-frequency resistance suggests the presence of a layer on the working electrode when the insertion process occurs. This electrical equivalent model is universal and can be applied to other composite cathode materials which undergo structural change during intercalation. For a high lithium content ($x > 0.7$), the formation of very small particles made up of a $LiNbO_3$-like structure occurs and consequently the amorphization of the material is observed.

The formation of small particles of a new phase in the electrode may limit considerably the reversibility of the material. Charge-discharge cycling shows the limitations (namely capacity and potential vs. Li) of the use of such a material as the cathode in a lithium battery but the positive influence of grinding the particles of the electroactive material is clearly demonstrated.

## References


1. Permer L, Lunberg M (1989) J Solid State Chem 81: 21
2. Murphy DW, Greenblatt M, Cava RJ, Zahurak SM (1981) Solid State Ionics 5: 327
3. Renou MF (1994) Doctoral Dissertation. Université du Maine, Le Mans
4. Permer L (1991) J Chem Soc Chem Commun 1
5. Bohnke C, Bohnke O, Fourquet JL (1998 ) Mol Cryst Liq Cryst 311: 23
6. Bohnke C, Bohnke O, Vuillemin B (1993) Electrochim Acta 38: 1935
7. Ho C, Raistrick ID, Huggins RA (1980) J Electrochem Soc 127: 343
8. Bohnke O, Bohnke C, Robert G, Carquille B (1982) Solid State Ionics 6: 121
9. Permer L, Lundberg M (1989) J Less-Common Met 156: 145
10. Levi MD, Salitra G, Markovsky B, Teller H, Aurbach D, Heider U, Heider L (1999) J Electrochem Soc 146: 1279